Supporting Information

Occurrence and Ecological Risk of Sunscreen-Derived Metallic and Plastic Particles in Marine Environments

Jiale Wang [1,†], Ruyi Lan [1,†], Ping Wang [2], Zhuomiao Liu [1,*], Ziyi Wang [1], Mengyao Tao [1], Meng Wang [1] and Jian Zhao [1,3,*]

[1] Frontiers Science Center for Deep Ocean Multispheres and Earth System, Institute of Coastal Environmental Pollution Control, Key Laboratory of Marine Environment and Ecology, Ocean University of China, Qingdao 266100, China
[2] Business School, Qingdao University, Qingdao 266100, China
[3] Laboratory for Marine Ecology and Environmental Science, Qingdao Marine Science and Technology Center, Qingdao 266237, China
* Correspondence: zhuomiaol@ouc.eu.cn (Z.L.); jzhao@ouc.edu.cn (J.Z.)
† These authors contributed equally to this work.

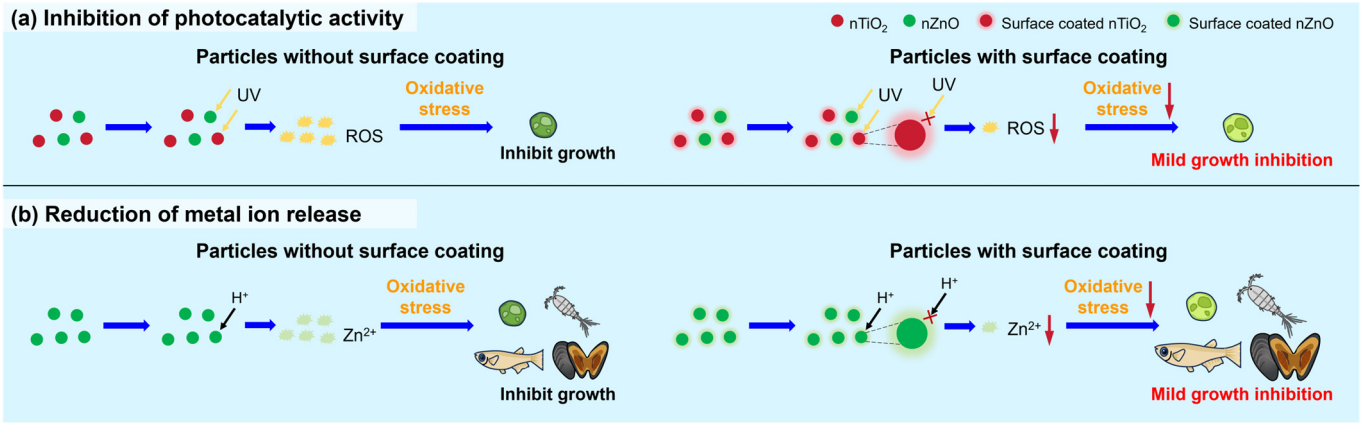

Figure S1. Effects of surface coatings on the toxicity of sunscreen-derived particles. (a): Inhibition of photocatalytic activity of particles. (b): Reduction of metal ion release from particles.

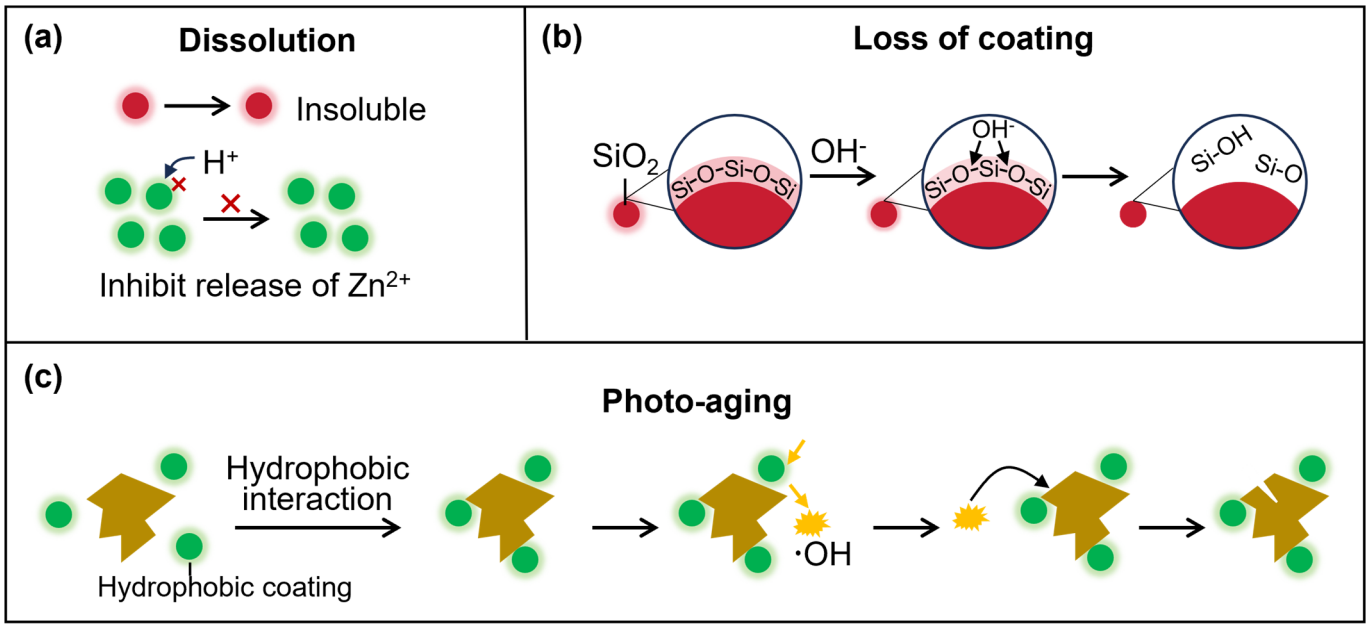

Figure S2. Transformation of sunscreen-derived particle with surface coating. (a): Dissolution of metallic nanoparticles. (b): Loss of surface coatings from metallic nanoparticle. (c): MNP photo-aging under coexist with metallic nanoparticles.

Table S1. The type and function of particles in sunscreens.

ID	Sun protection Factor	Particle Type	Particle Content	Particle Size (nm)	Particle Shape	Particle Function	Ref.
1	50	nZnO	14.5%	Length: 128 ± 51, Width: 51 ± 20	Rod	UV filter agent	[1]
2	20	nZnO	5%	136 ± 66	Amorphous	UV filter agent	
3	50	$nTiO_2$	2.4%	40 ± 25	Irregular, spherical	UV filter agent	
4	≥30	$nTiO_2$	2.4%	Length: 25.3 ± 8.8, Width: 51 ± 20	Needle	UV filter agent	[2]
		Al_2O_3	-	-	-	Coating	
		SiO_2	-	-	-	Coating	
5	≥30	$nTiO_2$	9.1%	Length: 24.6 ± 9.9, Width: 7.3 ± 1.8	Needle	UV filter agent	
		Al_2O_3	-	-		Coating	
6	≥30	$nTiO_2$	1.2%	Length: 24.9 ± 11.0, Width: 10.2 ± 3.9	Needle	UV filter agent	
		Al_2O_3	-	-	-	Coating	
		SiO_2	-	-	-	Coating	
7	≥30	nZnO	6.86%	Length: 78.5 ± 50.7, Width: 40.04 ± 29.7	Rod	UV filter agent	
8	≥30	nZnO	6.86%	Length: 79.9 ± 51.6, Width: 33.4 ± 20.3	Rod	UV filter agent	
9	≥30	nZnO	6.0%	Length: 81.3 ± 57.2, Width: 38.2 ± 28.7	Rod	UV filter agent	
		SiO_2	-	-	-	Coating	
10	≥30	$nTiO_2$	5.0%	Length: 67.0 ± 50.5, Width: 27.0 ± 24.1	Needle		
		nZnO	10.0%		Rod	UV filter agent	
11	30	$nTiO_2$	4.1%	Length: 19.9 ± 6.7, Width: 14.2 ± 5.0	Spherical, irregular	UV filter agent	[3]
12	50	$nTiO_2$	6.1%	Length: 23.4 ± 7.2, Width: 15.0 ± 4.8	Spherical, angular	UV filter agent	
13	30	$nTiO_2$	5.5%	Length: 35.5 ± 12.0, Width: 15.9 ± 3.9	Ellipsoidal, angular	UV filter agent	
		SiO_2	-	-	-	-	
14	30	$nTiO_2$	4.0%	Length: 13.4 ± 3.1, Width: 7.5 ± 1.7	Spherical	UV filter agent	
15	50	$nTiO_2$	4.1%	Length: 36.6 ± 11.6, Width: 7.3 ± 2.5	Elongated	UV filter agent	
16	50	$nTiO_2$	5.2%	Length: 24.2 ± 6.6, Width: 15.0 ± 4.3	Spherical	UV filter agent	
17	50	$nTiO_2$	6.0%	Length: 32.5 ± 12.1, Width: 13.9 ± 3.7	Ellipsoidal	UV filter agent	
		SiO_2	-	-	-	-	
18	50	$nTiO_2$	5.5%	Length: 29.3 ± 10.0, Width: 9.3 ± 3.7	Elongated, spherical, ellipsoidal	UV filter agent	
		SiO_2	-	-	-	-	
19	30	$nTiO_2$	13.1%	Length: 42.0 ± 12.5, Width: 22.7 ± 7.5	Spherical, angular, elongated	UV filter agent	
		Al_2O_3	-	-	-	Coating	
20	50	$nTiO_2$	5.9%	Length: 48.8 ± 16.6, Width: 31.5 ± 12.6	Spherical	UV filter agent	
		nZnO	-	-	-	UV filter agent	
21	50	$nTiO_2$	6.4%	Length: 27.0 ± 11.4, Width: 12.4 ± 3.9	Ellipsoidal, spherical	UV filter agent	
		SiO_2	-	-	-	Coating	
22		$nTiO_2$	3.1%	20–165	Spherical	UV filter agent	[4]
		nZnO	4.0%		Rod, varied		
23		$nTiO_2$	17.3%	40–240	Spherical	UV filter agent	
		nZnO	20.0%		Varied		
24		$nTiO_2$	8.0%	15–115	Rod	UV filter agent	
		nZnO	3.8%		Spherical		
25		$nTiO_2$	6.4%	18–115	Rod	UV filter agent	
		nZnO	6.0%		Spherical		
26		$nTiO_2$	9.0%	11–110	Rod	UV filter agent	
		nZnO	3.5%		Varied		

27		$nTiO_2$	9.0%	22–123	Rod	UV filter agent	
		nZnO	3.0%		Spherical		
28		$nTiO_2$	6.0%	15–250	Spherical	UV filter agent	
		nZnO	6.0%		Varied		
29		$nTiO_2$	8.0%	18–350	Spherical	UV filter agent	
		nZnO	2.5%		Varied		
30		$nTiO_2$	0.67%	14–145	Rod	UV filter agent	
		nZnO	11.6%		Spherical		
31		$nTiO_2$	7.5%	20–170	Rod	UV filter agent	
		nZnO	5.0%		Varied		
32	30	$nTiO_2$	1.9%	Length: 46.5–93.6, Width: 13.5–25.9	Spherical, rod, irregular	UV filter agent	
		Al_2O_3	-	-	-	Coating	
		SiO_2	-	-	-	Coating	
33	40	$nTiO_2$	0.6%	Length: 48.5–81.7, Width: 9.8–16.9	Spherical, rod, irregular	UV filter agent	[5]
		Al_2O_3	-	-	-	Coating	
		SiO_2	-	-	-	Coating	
34	50	$nTiO_2$	0.5%	Length: 44.4–69.2, Width: 10.6–14.4	Spherical, rod	UV filter agent	
		Al_2O_3	-	-	-	Coating	
		SiO_2	-	-	-	Coating	
35	50+	nZnO	2.99%	23.57 ± 5.52	Spherical	UV filter agent	[6]
				Length: 50.97 ± 12.48, Width: 16.73 ± 3.70	Rod		
		Acrylate copolymer, silicone-based cross-polymer	~5.2%	5540	Spherical	Emulsion facilitation, viscosity control	
36		$nTiO_2$	-	27.9 ± 7.0	Needle	UV filter agent	[7]
		nZnO	2.25%	27.9 ± 8.8	Roundish		
37		$nTiO_2$	-	24.9 ± 9.1	Roundish	UV filter agent	
38		$nTiO_2$	-	23.9 ± 6.3	Roundish	UV filter agent	
39		$nTiO_2$	15.35%	45.7 ± 14.0	Needle	UV filter agent	[8]
40		$nTiO_2$	13.84%	33.7 ± 11.4	Round	UV filter agent	
		nZnO	4.43%	>100	Varied		
41		$nTiO_2$	-	39.5 ± 14.0	Needle	UV filter agent	
		nZnO	3.35%	33.5 ± 20.7	Varied		
42		$nTiO_2$	13.52%	49.6 ± 17.0	Needle	UV filter agent	
		nZnO	5%	86.9 ± 32.1	Roundish		
43		$nTiO_2$	13.99%	35.1 ± 10.7	Roundish	UV filter agent	
44		$nTiO_2$	-	42.5 ± 12.6	Needle	UV filter agent	
		nZnO	4%	11.4 ± 5.5	Roundish		
45		$nTiO_2$	13.01%	30.9 ± 10.6	Varied	UV filter agent	
		nZnO	4.99%	>100	Varied		
46		$nTiO_2$	12.47%	>100	Varied	UV filter agent	
47		$nTiO_2$	9.5%	24.5 ± 8.1	Roundish	UV filter agent	
48	50+	EMA-MMA, hybrid silicone powder	-	6870	Spherical	Improve texture and water resistance	[9]
49	50+	PMMA, LMA-GDMA	-	6150	Spherical	Improve texture and water resistance	
50	50+	LMA-based polymer	-	2780	Spherical	Improve texture and water resistance	

Abbreviations of polymers: EMA-MMA: Ethylene glycol dimethacrylate-methyl methacrylate copolymer; PMMA: Poly(methyl methacrylate); LMA-GDMA: Lauryl methacrylate/glycol dimethacrylate crosspolymer; LMA: Lauryl methacrylate.

Table S2. Advantages and disadvantages of extraction approaches for metallic nanoparticles and MNPs from sunscreens, seawater and sediments.

Particles	Extraction Approaches	Recovery Rate	Advantages	Disadvantages	Applicable Samples	Ref.
Metallic nanoparticles	Organic solvent combined with centrifugation	78.0-98.0%	- Less sample loss - Applicable to large-batch samples	- Poor reproducibility limited by organic components	Sunscreens	[1,3]
	Organic solvent combined with ultrafiltration	52.0-96.0%	- Collection of particles in specific size	- Not applicable to large-batch samples - Cause sample loss	Sunscreens	[1,3]
	Cloud point extraction	88.1 ± 9.6%	- High enrichment efficiency for trace-level particles	- Time-consuming extraction - Not applicable to large-batch samples	Seawater	[10]
	DI water combined with sedimentation	66.3 ± 2.0%	- Operational procedures are simple	- Low recovery - Time-consuming extraction	Sediments	[11,12]
	DI water combined with centrifugation	76.3 ± 4.3%	- Time-saving extraction	- Low recovery for small particle size (e.g., 30 nm)	Sediments	[12,13]
MNPs	Organic solvent combined with centrifugation	-	- Operational procedures are simple	- Morphological damage of particles	Sunscreens	[6,9]
	Gradient filtration	MPs (1 μm): 80.2-102.0%; NPs: (50 nm) ~ 93.0%	- Operational procedures are simple - Collection of particles in specific size	- Low efficiency limited by NOM - Time-consuming extraction	Seawater	[14–16]
	Density separation	NaCl: 68.0 ± 3.0%; $ZnCl_2$: 85.0 ± 2.0%; $CaCl_2$: 90.0 ± 1.0%	- High recovery for MPs - NaCl is non-toxic and inexpensive - $ZnCl_2$ and $CaCl_2$ are applicable to high-density MPs	- NaCl is not applicable to high-density MPs (e.g., PET, PVC) - $ZnCl_2$ is harmful and corrosive - Time-consuming extraction - Not applicable to NPs	Sediments	[17–19]
	Dichloromethane combined with centrifugation	NPs: 75.0-93.0%	- High recovery for NPs	- Morphological damage of particles	Sediments	[20,21]

Table S3. Advantages and disadvantages of detection techniques for sunscreen-derived metallic nanoparticles and MNPs.

Techniques	Qualitative Analysis	Quantitative Analysis	Morphology	Detection Limits	Advantages	Disadvantages	Applicable Particles	Ref.
SEM	No	Yes	Yes	50 nm	- Analysis of surface morphology	- No elemental composition information without EDS - Complex sample preparation	MNPs	[22]
TEM	No	Yes	Yes	20 nm	- High resolution - Analysis of morphology	- No elemental composition information without EDS - Complex sample preparation	NPs and metallic nanoparticles	[23]
HRTEM	Yes	Yes	Yes	1 nm	- Ultra-high resolution - Analysis of crystal structure	- Complex sample preparation	NPs and metallic nanoparticles	[24]
XPS	Yes	No	No	-	- Determination of elemental composition and chemical state	- Only analysis of the sample surface layer	MNPs and metallic nanoparticles	[25]
XRD	Yes	No	No	-	- Determination of crystal phase and crystallinity	- Not applicable to amorphous substance	MNPs and metallic nanoparticles	[8]
ATR-FTIR	Yes	No	No	20 μm	- Rapid identification of MP chemical composition	- Not applicable to metallic nanoparticles - Susceptible to water interference	MPs	[26,27]
μ-Raman	Yes	Yes	No	1 μm	- High resolution - Identification of individual MP chemical composition - Quantification of particle concentration	- Not applicable to NPs - No mass concentration information - Susceptible to fluorescence interference	MPs	[28]
μ-FTIR	Yes	Yes	No	10 μm	- Identification of individual MP chemical composition - Quantification of particle concentration - Non-destructive analysis	- Not applicable to NPs - No mass concentration information - Susceptible to water interference	MPs	[29]
Py-GC/MS	Yes	Yes	No	0.003 μg	- Simultaneous determination of polymer type and mass concentration	- No particle concentration information - Destructive analysis - Susceptible to interference from environmental matrices	MNPs	[30]
ICP-MS	Yes	Yes	No	17 ng/L	- High sensitivity - Rapid determination of element concentrations	- No particle concentration information	Metallic elements	[31]
sp-ICP-MS	Yes	Yes	No	Size: 20 nm; concentration: 35 particles/mL	- High sensitivity - Rapid determination of particle concentration and size distribution	- Not applicable to MNPs without metal-labeling	Metallic nanoparticles	[12,32]
sp-ICP-TOF-MS	Yes	Yes	No	Size: 7 nm; concentration: 0.03 fg	- High sensitivity - Simultaneous detection of multiple elements and isotopes in single particle	- High instrument cost	Metallic nanoparticles	[33,34]

Abbreviations of Techniques: SEM: Scanning electron microscopy; TEM: Transmission electron microscopy; HRTEM: High-resolution transmission electron microscopy ;XPS: X-ray photoelectron spectroscopy; XRD: X-ray diffraction; ATR-FTIR: Attenuated total reflectance-Fourier transform infrared spectroscopy; μ-Raman: Micro-Raman spectroscopy; μ-FTIR: Micro-Fourier transform infrared spectroscopy; Py-GC/MS: Pyrolysis coupled with gas chromatography and mass spectrometry; ICP-MS: Inductively coupled plasma mass spectrometry; sp-ICP-MS: Single-particle inductively coupled plasma mass spectrometry; sp-ICP-TOF-MS: Single-particle inductively coupled plasma time-of-flight mass spectrometry.

Table S4. Occurrence of sunscreen-derived metallic nanoparticles in beach seawater.

Area		Particles Type	Concentration/ Emissions	Analysis Method	Ref.
Marseille, French	La Lave Beach	$nTiO_2$ nZnO	13.8–152.9 μg/L 0–14.8 μg/L	Seting sampling points in bathing zone and beyond bathing zone	[35]
	Prophète Beach	$nTiO_2$ nZnO	117.9–903.1 μg/L 0–11.2 μg/L		
	Pointe Rouge Beach	$nTiO_2$ nZnO	6.0–8.6 μg/L -		
Majorca Island, Spain	Palmira Beach	Ti element Zn element	37.6 ± 7.3 μg/L 3.3 μg/L	Seting sampling points in densely populated beaches and an open and scarcely used beach	[36]
	Santa Ponça Beach	Ti element Zn element	12.1 ± 1.2 μg/L 10.8 μg/L		
Hérault, France	Palavas-les-Flots Beach	$nTiO_2$	Max: 269.2 μg/L	Positive correlation between concentration and the number of beach tourists is presented	[37]
Marseille, French		$nTiO_2$ nZnO	211 mg/person/day 28 mg/person/day	Estimate emissions based on survey questionnaires	[35]
Global reef areas		$nTiO_2$	36–56 t/year	Estimating emissions through laboratory simulations	[38]

Table S5. Toxicity endpoints of marine species for $nTiO_2$ and nZnO.

Particles Type	Size (nm)	Dose Descriptor	Test Organism	Concentration (μg/L)	Exposure Time (h)	AF time[a]	AF No-Effect[b]	Species Sensitivity (μg/L)	Ref.
$nTiO_2$	20	NOEC	*Acropora* spp.	6300	24	10	1	630	[39]
$nTiO_2$	34.9 ± 5.5	EC_{50}	*Alexandrium tamarense*	85,080	72	1	10	8508	[40]
$nTiO_2$	21	LC_{50}	*Artemia franciscana*	15,000	96	10	10	150	[41]
$nTiO_2$	10–30	NOEC	*Artemia salina*	100,000	24	10	1	10,000	[42]
$nTiO_2$	18.3 ± 3.2	EC_{50}	*Artemia salina*	120,900	48	10	10	1209	[43]
$nTiO_2$	20.2 ± 6.44	LC_{50}	*Artemia* sp.	18,940	48	10	10	189.4	[44]
$nTiO_2$	25	EC_{50}	*Brachionus plicatilis*	10,430	48	10	10	104.3	[45]
$nTiO_2$	32	EC_{50}	*Brachionus plicatilis*	267,300	48	10	10	2673	[45]
$nTiO_2$	<100	LOEC	*Chaetoceros gracilis*	1000	75	1	2	500	[46]
$nTiO_2$	25	EC_{50}	*Chaetoceros muelleri*	50,000	360	1	10	5000	[47]
$nTiO_2$	10–25	LC_{50}	*Chaetoceros muelleri*	5010	240	1	10	501	[48]
$nTiO_2$	21	EC_{50}	*Chlorella pyrenoidosa*	132,900	96	1	10	13,290	[49]
$nTiO_2$	24.6 ± 4.5	LC_{50}	*Dunaliella salina*	11,350	48	1	10	1135	[50]
$nTiO_2$	25	NOEC	*Dunaliella tertiolecta*	7500	96	1	1	7500	[51]
$nTiO_2$	25	NOEC	*Dunaliella tertiolecta*	7500	96	1	1	7500	[52]
$nTiO_2$	15–30	NOEC	*Dunaliella tertiolecta*	3000	96	1	2	1500	[53]
$nTiO_2$	15–30	LOEC	*Isochrysis galbana*	1000	96	1	2	500	[53]
$nTiO_2$	<25	EC_{50}	*Isochrysis galbana*	50,000	96	10	10	500	[54]
$nTiO_2$	19.1 ± 6.7	NOEC	*Magallana gigas*	100	72	10	1	10	[55]
$nTiO_2$	8.33–49.58	LC50	Moina mongolica	4140	72	1	10	414	[56]
$nTiO_2$	25 ± 5	LOEC	*Mytilus coruscus*	2500	336	10	2	125	[57]
$nTiO_2$	25 ± 5	LOEC	*Mytilus coruscus*	2500	336	10	2	125	[58]
$nTiO_2$	22	NOEC	*Mytilus galloprovincialis*	5000	24	10	1	500	[59]
$nTiO_2$	21	LOEC	*Mytilus galloprovincialis*	10,000	96	10	2	500	[60]
$nTiO_2$	21	EC_{50}	*Nitzschia closterium*	88,780	96	1	10	8878	[61]
$nTiO_2$	60	EC_{50}	*Nitzschia closterium*	11,880	96	1	10	1188	[61]
$nTiO_2$	21	LC_{50}	*Oryzias latipes*	8500	48	10	10	85	[62]
$nTiO_2$	21	EC_{50}	*Phaeodactylum tricornutum*	43	72	1	10	4.3	[63]
$nTiO_2$	21	EC_{20}	*Phaeodactylum tricornutum*	16,000	96	1	2	8000	[41]
$nTiO_2$	21	NOEC	Pocillopora damicornis	6210	24	10	1	621	[64]
$nTiO_2$	59.7	EC_{50}	*Skeletonema costatum*	117,000	72	1	10	11,700	[65]
$nTiO_2$	5.3	EC_{50}	*Skeletonema costatum*	353,300	72	1	10	35,330	[65]
$nTiO_2$	37.3	NOEC	*Thalassiosira pseudonana*	2500	96	1	1	2500	[66]
$nTiO_2$	15–30	LOEC	*Thalassiosira pseudonana*	3000	96	1	2	1500	[53]
nZnO	32.28 ± 13.30	LC_{50}	*Artemia franciscana*	4860	96	10	10	48.6	[67]
nZnO	<100	LC_{50}	*Artemia salina*	72,500	96	10	10	725	[68]
nZnO	80–200	LC_{50}	*Artemia salina*	12,140	12	10	10	121.4	[69]
nZnO	80–200	LC_{50}	*Artemia salina*	100,000	96	10	10	1000	[70]
nZnO	30 ± 10	LC_{50}	*Artemia salina*	95,600	96	10	10	956	[71]
nZnO	<50	LC_{50}	*Brachionus koreanus*	9903	24	10	10	99.03	[72]
nZnO	40–48	EC_{20}	*Chlorella vulgaris*	300,000	24	10	2	15,000	[73]

nZnO	30–40	LC_{50}	*Corophium insidiosum*	1750	96	10	10	17.5	[74]
nZnO	35 ± 10	LOEC	*Corophium volutator*	200	2400	1	2	100	[75]
nZnO	20–50	LOEC	*Crassostrea gigas*	40.7	24	10	2	20.35	[76]
nZnO	31.7 ± 13.0	LC50	Crassostrea gigas	37,200	96	10	10	372	[77]
nZnO	10–30	LC_{50}	*Dunaliella salina*	7630	24	10	10	76.3	[69]
nZnO	100	EC_{50}	*Dunaliella tertiolecta*	2500	96	1	10	250	[51]
nZnO	20–30	LOEC	*Dunaliella tertiolecta*	1000	96	1	1	1000	[78]
nZnO	< 100	EC_{50}	*Dunaliella tertiolecta*	1300	96	1	10	130	[79]
nZnO	< 100	EC_{10}	*Ficopomatus enigmaticus*	50	48	10	1	2.5	[63]
nZnO	< 100	LOEC	*Ficopomatus enigmaticus*	100	672	1	2	50	[80]
nZnO	30–40	LC_{50}	*Gammarus aequicauda*	300	96	10	10	3	[81]
nZnO	50 ± 10	EC_{20}	*Gymnodinium*	10,000	96	1	2	5000	[82]
nZnO	20–30	LOEC	*Isochrysis galbana*	1000	96	1	1	1000	[78]
nZnO	50 ± 10	EC_{50}	*Keletonema costatum*	3600	96	1	10	360	[83]
nZnO	30	LOEC	*Mytilus edulis*	10	504	10	2	0.5	[84]
nZnO	30.1 ± 0.4	LOEC	*Mytilus edulis*	81	336	10	2	4.05	[85]
nZnO	< 100	LC_{50}	*Mytilus galloprovincialis*	975	672	1	10	97.5	[86]
nZnO	20–30	EC_{50}	*Mytilus galloprovincialis*	1500	1728	1	10	150	[87]
nZnO	30 ± 10	EC10	Neomysis awatschensis	30	28	1	1	30	[71]
nZnO	30 ± 10	EC10	Oryzias melastigma	2820	28	1	1	2820	[71]
nZnO	40–50	LC_{50}	*Penaeus semisulcatus*	49,220	24	10	10	492.2	[88]
nZnO	26.2 ± 5.1	LC_{50}	*Skeletonema costatum*	2360	96	1	10	236	[89]
nZnO	26.2 ± 5.1	EC_{50}	*Skeletonema costatum*	1700	72	1	10	170	[65]
nZnO	26.2 ± 5.1	LC_{50}	*Skeletonema costatum*	18,660	24	10	10	186.6	[66]
nZnO	20–30	LOEC	*Skeletonema marinoi*	1000	96	1	2	500	[78]
nZnO	<100	EC_{50}	*Tetraselmis suesica*	2570	96	1	10	257	[79]
nZnO	<50 ± 5	EC_{50}	*Thalasiosira pseudonana*	50,000	96	1	10	5000	[90]
nZnO	26.2 ± 5.1	LC_{50}	*Thalassiosia pseudonana*	4560	96	1	10	456	[89]
nZnO	20	LC_{50}	*Thalassiosira pseudonana*	2500	96	1	10	250	[91]
nZnO	20–30	LOEC	*Thalassiosira pseudonana*	500	96	1	2	250	[78]
nZnO	20–30	LOEC	*Thalassiosira weissflogii*	94.2	168	1	2	47.1	[92]
nZnO	30–40	LC_{50}	*Tigriopus fulvus*	600	96	10	10	6	[74]
nZnO	24.95 ± 6.16	LC_{50}	*Tigriopus japonicus*	2400	96	10	10	24	[93]
nZnO	20–30	LC_{50}	*Tigriopus japonicus*	2440	96	10	10	24.4	[94]

[a]: Assessment factor, AF of 1 is used for for long-term studies, and AF of 10 is used for short-term studies; [b]: AF of 10 is used for LC_{50}/EC_{50}, AF of 2 is used for EC_{20} and LOEC, and an AF of 1 is used for NOEC and EC_{10}.

Table S6. Fitting parameters of species sensitivity distribution (SSD) for deriving predicted no effect concentration (PNECs) of sunscreen-derived particles.

Particles Type	Model	RMSE	R^2	*p*(A-D) [a]	PNEC(μg/L)
$nTiO_2$	Normal	0.055	0.983	>0.05	54.53
nZnO	Normal	0.027	0.988	>0.05	3.90

Abbreviations: RMSE: Root mean squared error. [a]: *p* value of Anderson-Darling test.

Table S7. The transformation pathways of sunscreen-derived particles in marine environments.

Particle Type	Condition	Transformation Pathway	Transformation Results	Mechanisms	Ref.
nZnO	- Artificial seawater (pH~8.2) - 1 h	Dissolution	Dissolution of nZnO: 24%	$ZnO + H_2O \rightarrow Zn^{2+} + 2OH^-$	[95]
nZnO	- Artificial seawater (pH~8.1) - 24 h	Dissolution	Dissolution of nZnO: 25-44%	$ZnO + H_2O \rightarrow Zn^{2+} + 2OH^-$	[96]
nZnO	- Aqueous solutions (pH 8.5-8.6, ionic strength 0.1 M) - NOM (Suwannee River humic acid), - 70 min	Dissolution	Dissolution of nZnO increased from 4 to 25 μM as NOM concentration increased from 0 to 40 mg C/L	NOM enhances the dissolution of nZnO by complexing with Zn^{2+}	[97]
nZnO	- Artificial seawater - 7 d	Form secondary species	35.6-38.0% of nZnO transformed into zinc sulfide, and 16.9-17.8% of nZnO transformed into zinc phosphate	nZnO directly interacts with sulfur and phosphorus, resulting in transformation into zinc sulfide and zinc phosphate	[98]
nZnO	- Natural seawater - 7 d	Form secondary species	11.8-17.1% of nZnO transformed into zinc sulfide	NOM coats nZnO and produces steric hindrance, which preferentially inhibits the formation of zinc phosphate, while the formation of ZnS is kinetically preferred and still occurs slightly	[98]
PMMA plates	- Seawater - 36-month immersion	Physical fragmentation	69% reduction in tensile strength	Water disrupts hydrogen bonds and van der Waals forces within the macromolecular network	[99]
EMA-MMA copolymer	- Ultrapure water - Stirring (1000 rpm) - 84 h	Mechanical fragmentation	20% reduction in size	Physical rupture under mechanical stress	[9]
EMA-MMA copolymer	- Ultrapure water - Sunlight irradiation (UVA-13.6 and UVB-3 W/m^2) - Stirring (1000 rpm) - 84 h	Photochemical degradation and mechanical fragmentation	35% reduction in size, and 1.2-fold increase in carbonyl ratio	Photoirradiation induces random homolytic scission of the main-chain C=C bond of poly MMA, leading to the formation of polymeric alcohols	[9]
Acrylate copolymer	- Ultrapure water - Sunlight irradiation (1000 W/m^2) - nZnO (14 mg/mL) - 12 h	Photochemical degradation	MPs complete breakup to several pieces after 9 h, and the carbonyl ratio reached 50.59% after 12 h	nZnO produces hydroxyl radicals under light irradiation, thereby promoting the oxidative degradation of MNPs	[6]
PMMA MPs	- Natural seawater (pH~8.2) - UV irradiation (275-470 nm, 240 W) - 120 h	Photochemical degradation	MPs (16-2000 μm) fragmented into smaller sizes, while the 50-125 μm fraction increased twofold, and 25% increase of oxidation index	The energy of UV radiation is sufficient to break the C-C and C-H bonds and activate oxygen molecules, resulting in the generation of additional oxygen-containing functional groups	[100]
PMMA films	- Minimal media - Marine microorganisms (*Aspergillus* sp.) - 6 weeks	Biodegradation	16% weight loss	Not mentioned	[101]
PMMA/cellulose films	- Minimal media, - Marine microorganisms (*Aspergillus* sp.) - 6 weeks	Biodegradation	24% weight loss	Not mentioned	[101]

Abbreviations of Techniques: PMMA: Polymethyl methacrylate; EMA-MMA: Ethyl methylacrylate-methyl methacrylate.

References

1. Hanigan, D.; Truong, L.; Schoepf, J.; et al. Trade-offs in ecosystem impacts from nanomaterial versus organic chemical ultraviolet filters in sunscreens. *Water Res*. **2018**, *139*, 281–290.
2. Lewicka, Z.A.; Benedetto, A.F.; Benoit, D.N.; et al. The structure, composition, and dimensions of TiO_2 and ZnO nanomaterials in commercial sunscreens. *J. Nanopart. Res.* **2011**, *13*, 3607–3617.
3. Philippe, A.; Košík, J.; Welle, A.; et al. Extraction and characterization methods for titanium dioxide nanoparticles from commercialized sunscreens. *Environ. Sci. Nano* **2018**, *5*, 191–202.
4. Bairi, V.G.; Lim, J.-H.; Fong, A.; et al. Size characterization of metal oxide nanoparticles in commercial sunscreen products. *J. Nanopart. Res*. **2017**, *19*, 256.
5. Nthwane, Y.B.; Tancu, Y.; Maity, A.; et al. Characterisation of titanium oxide nanomaterials in sunscreens obtained by extraction and release exposure scenarios. *SSN Appl. Sci.* **2019**, *1*, 312.
6. Sun, A.; Wang, W. Photodegradation of microplastics by ZnO nanoparticles with resulting cellular and subcellular responses. *Environ. Sci. Technol*. **2023**, *57*, 8118–8129.
7. Lu, P.J.; Cheng, W.L.; Huang, S.C.; et al. Characterizing titanium dioxide and zinc oxide nanoparticles in sunscreen spray. *Int. J. Cosmet. Sci.* **2015**, *37*, 620–626.
8. Lu, P.J.; Fang, S.W.; Cheng, W.L.; et al. Characterization of titanium dioxide and zinc oxide nanoparticles in sunscreen powder by comparing different measurement methods. *J. Food Drug Anal*. **2018**, *26*, 1192–1200.
9. Sun, A.; Wang, W. Photodegradation controls of potential toxicity of secondary sunscreen-derived microplastics and associated leachates. *Environ. Sci. Technol*. **2025**, *59*, 5223–5236.
10. Yang, Y.; Liu, X.; Luo, L.; et al. Quantitative detection of zinc oxide nanoparticle in environmental water by cloud point extraction combined ICP-MS. *Adsorpt. Sci. Technol.* **2021**, *2021*, 9958422.
11. Tou, F.; Niu, Z.; Fu, J.; et al. Simple method for the extraction and determination of Ti-, Zn-, Ag-, and Au-containing nanoparticles in sediments using single-particle inductively coupled plasma mass spectrometry. *Environ. Sci. Technol*. **2021**, *55*, 10354–10364.
12. Li, G.; Liu, X.; Wang, H.; et al. Detection, distribution and environmental risk of metal-based nanoparticles in a coastal bay. *Water Res*. **2023**, *242*, 120242.
13. Choleva, T.G.; Tsogas, G.Z.; Vlessidis, A.G.; et al. Development of a sequential extraction and speciation procedure for assessing the mobility and fractionation of metal nanoparticles in soils. *Environ. Pollut.* **2020**, *263*, 114407.
14. Li, Q.; Lai, Y.; Yu, S.; et al. Sequential isolation of microplastics and nanoplastics in environmental waters by membrane filtration, followed by cloud-point extraction. *Anal. Chem.* **2021**, *93*, 4559–4566.
15. Wu, Z.; Qin, M.; Wei, H. Improved reliability of Raman spectroscopic imaging of low-micrometer microplastic mixtures in lake water by fractionated membrane filtration. *ACS ES&T Water* **2023**, *3*, 2616–2626.
16. Arnould, M.; Quingongo, R.; Albignac, M.; et al. A membrane cascade for size-based separation and concentration of nanoplastics in environmental waters. *Sep. Purif. Technol.* **2025**, *373*, 133352.
17. Cutroneo, L.; Reboa, A.; Geneselli, I.; et al. Considerations on salts used for density separation in the extraction of microplastics from sediments. *Mar. Pollut. Bull.* **2021**, *166*, 112216.
18. Nabi, I.; Zhang, L. A review on microplastics separation techniques from environmental media. *J. Cleaner Prod.* **2022**, *337*, 130458.
19. Gran, A.; Vidal-Barrachina, D.; Casado-Coy, N.; et al. Comparing methods for optimising microplastic extraction in sediment through density separation. *Environ. Pollut*. **2025**, *383*, 126894.
20. Li, Z.; Gao, Y.; Wu, Q.; et al. Quantifying the occurrence of polystyrene nanoplastics in environmental solid matrices via pyrolysis-gas chromatography/mass spectrometry. *J. Hazard. Mater.* **2022**, *440*, 129855.
21. Li, P.; Lai, Y.; Zheng, R.-g.; et al. Extraction of common small microplastics and nanoplastics embedded in environmental solid matrices by tetramethylammonium hydroxide digestion and dichloromethane dissolution for Py-GC-MS determination. *Environ. Sci. Technol*. **2023**, *57*, 12010–12018.
22. Wang, Z.; Wang, Y.; Lu, X.; et al. Generation of simulated "Natural" nanoplastics from polypropylene food packaging as the experimental standard. *Molecules* **2023**, *28*, 7254.
23. Sökmen, T.Ö.; Sulukan, E.; Türkoğlu, M.; et al. Polystyrene nanoplastics (20 nm) are able to bioaccumulate and cause oxidative DNA damages in the brain tissue of zebrafish embryo (*Danio rerio*). *Neurotoxicology* **2020**, *77*, 51–59.
24. Gumbiowski, N.; Barthel, J.; Loza, K.; et al. Simulated HRTEM images of nanoparticles to train a neural network to classify nanoparticles for crystallinity. *Nanoscale Adv.* **2024**, *6*, 4196–4206.
25. Giulio, D.T.; Malitesta, C.; Mazzotta, E. Surface chemical analysis of plastic materials by X-ray photoelectron spectroscopy: Understanding weathering, fragmentation and contaminant uptake in marine environments. *Macromol. Mater. Eng*. **2026**, *311*, e00280.
26. Nor, N.H.M.; Obbard, J.P. Microplastics in Singapore's coastal mangrove ecosystems. *Mar. Pollut. Bull*. **2014**, *79*, 278–283.
27. Al-Saeedi, F.M.A.A.; Dahmash, E.Z. *In vitro* assessment of sunscreen efficacy using fourier transform infrared (FTIR) spectroscopy on synthetic skin. *AAPS PharmSciTech* **2022**, *23*, 73.

28. Imhof, H.K.; Schmid, J.; Niessner, R.; et al. A novel, highly efficient method for the separation and quantification of plastic particles in sediments of aquatic environments. *Limnol. Oceanogr.:Methods* **2012**, *10*, 524–537.
29. Yang, J.; Monnot, M.; Sun, Y.; et al. Microplastics in different water samples (seawater, freshwater, and wastewater): Methodology approach for characterization using micro-FTIR spectroscopy. *Water Res.* **2023**, *232*, 119711.
30. Hermabessiere, L.; Himber, C.; Boricaud, B.; et al. Optimization, performance, and application of a pyrolysis-GC/MS method for the identification of microplastics. *Anal. Bioanal. Chem.* **2018**, *410*, 6663–6676.
31. Wang, Y.; Chen, B.; Wang, B.; et al. Phosphoric acid functionalized magnetic sorbents for selective enrichment of TiO_2 nanoparticles in surface water followed by inductively coupled plasma mass spectrometry detection. *Sci. Total Environ.* **2020**, *703*, 135464.
32. Azimzada, A.; Farner, J.M.; Hadioui, M.; et al. Release of TiO_2 nanoparticles from painted surfaces in cold climates: characterization using a high sensitivity single-particle ICP-MS. *Environ. Sci. Nano* **2020**, *7*, 139–148.
33. Naasz, S.; Weigel, S.; Borovinskaya, O.; et al. Multi-element analysis of single nanoparticles by ICP-MS using quadrupole and time-of-flight technologies. *J. Anal. At. Spectrom.* **2018**, *33*, 835–845.
34. Barabash, M.; Ahabchane, H.E.; Hadioui, M.; et al. Release of TiO_2 and ZnO nanoparticles from sunscreens into natural waters: detection and discrimination from natural particles using SP ICP-ToF-MS. *Environ. Sci. Nano* **2025**, *12*, 4994–5007.
35. Labille, J.; Slomberg, D.; Catalano, R.; et al. Assessing UV filter inputs into beach waters during recreational activity: A field study of three French Mediterranean beaches from consumer survey to water analysis. *Sci. Total Environ.* **2020**, *706*, 136010.
36. Tovar-Sánchez, A.; Sánchez-Quiles, D.; Basterretxea, G.; et al. Sunscreen products as emerging pollutants to coastal waters. *PLoS One* **2013**, *8*, e65451.
37. Thallinger, D.; Labille, J.; Milinkovitch, T.; et al. UV filter occurrence in beach water of the Mediterranean coast – A field survey over 2 years in Palavas-les-Flots, France. Int. *J. Cosmetic Sci.* **2023**, *45*, 67–83.
38. Botta, C.; Labille, J.; Auffan, M.; et al. TiO_2-based nanoparticles released in water from commercialized sunscreens in a life-cycle perspective: Structures and quantities. *Environ. Pollut.* **2011**, *159*, 1543–1550.
39. Corinaldesi, C.; Marcellini, F.; Nepote, E.; et al. Impact of inorganic UV filters contained in sunscreen products on tropical stony corals (*Acropora* spp.). *Sci. Total Environ.* **2018**, *637*, 1279–1285.
40. Li, M.; Jiang, Y.; Chuang, C.-Y.; et al. Recovery of *Alexandrium tamarense* under chronic exposure of TiO_2 nanoparticles and possible mechanisms. *Aquat. Toxicol.* **2019**, *208*, 98–108.
41. Minetto, D.; Libralato, G.; Marcomini, A.; et al. Potential effects of TiO_2 nanoparticles and $TiCl_4$ in saltwater to *Phaeodactylum tricornutum* and *Artemia franciscana*. *Sci. Total Environ.* **2017**, *579*, 1379–1386.
42. Ates, M.; Daniels, J.; Arslan, Z.; et al. Effects of aqueous suspensions of titanium dioxide nanoparticles on *Artemia salina*: Assessment of nanoparticle aggregation, accumulation, and toxicity. *Environ. Monit. Assess.* **2013**, *185*, 3339–3348.
43. Bhuvaneshwari, M.; Sagar, B.; Doshi, S.; et al. Comparative study on toxicity of ZnO and TiO_2 nanoparticles on Artemia salina: Effect of pre-UV-A and visible light irradiation. *Environ. Sci. Pollut. Res.* **2017**, *24*, 5633–5646.
44. Rekulapally, R.; Chavali, L.N.M.; Idris, M.M.; et al. Toxicity of TiO_2, SiO_2, ZnO, CuO, Au and Ag engineered nanoparticles on hatching and early nauplii of *Artemia* sp. *PeerJ* **2019**, *6*, e6138.
45. Clément, L.; Hurel, C.; Marmier, N. Toxicity of TiO_2 nanoparticles to cladocerans, algae, rotifers and plants – Effects of size and crystalline structure. *Chemosphere* **2013**, *90*, 1083–1090.
46. Sendra, M.; Sánchez-Quiles, D.; Blasco, J.; et al. Effects of TiO_2 nanoparticles and sunscreens on coastal marine microalgae: Ultraviolet radiation is key variable for toxicity assessment. *Environ. Int.* **2017**, *98*, 62–68.
47. Baharlooeian, M.; Kerdgari, M.; Shimada, Y. Ecotoxicological effects of TiO_2 nanoparticulates and bulk Ti on microalgae *Chaetoceros muelleri*. *Environ. Technol. Innov.* **2021**, *23*, 101720.
48. Bameri, L.; Sourinejad, I.; Ghasemi, Z.; et al. Toxicity of TiO_2 nanoparticles to the marine microalga *Chaetoceros muelleri* Lemmermann, 1898 under long-term exposure. *Environ. Sci. Pollut. Res.* **2022**, *29*, 30427–30440.
49. Zhu, L.; Booth, A.M.; Feng, S.; et al. UV-B radiation enhances the toxicity of TiO_2 nanoparticles to the marine microalga *Chlorella pyrenoidosa* by disrupting the protection function of extracellular polymeric substances. *Environ. Sci. Nano* **2022**, *9*, 1591–1604.
50. Bhuvaneshwari, M.; Thiagarajan, V.; Nemade, P.; et al. Toxicity and trophic transfer of P25 TiO_2 NPs from *Dunaliella salina* to *Artemia salina*: Effect of dietary and waterborne exposure. *Environ. Res.* **2018**, *160*, 39–46.
51. Schiavo, S.; Oliviero, M.; Miglietta, M.; et al. Genotoxic and cytotoxic effects of ZnO nanoparticles for *Dunaliella tertiolecta* and comparison with SiO_2 and TiO_2 effects at population growth inhibition levels. *Sci. Total Environ.* **2016**, *550*, 619–627.
52. Manzo, S.; Buono, S.; Rametta, G.; et al. The diverse toxic effect of SiO_2 and TiO_2 nanoparticles toward the marine microalgae *Dunaliella tertiolecta*. *Environ. Sci. Pollut. Res.* **2015**, *22*, 15941–15951.
53. Miller, R.J.; Bennett, S.; Keller, A.A.; et al. TiO_2 nanoparticles are phototoxic to marine phytoplankton. *PLoS One* **2012**, *7*, e30321.
54. Sivakumar, M.; Dhinakarasamy, I.; Chakraborty, S.; et al. Effects of titanium oxide nanoparticles on growth, biochemical composition, and photosystem mechanism of marine microalgae *Isochrysis galbana* COR-A3. *Nanotoxicology* **2025**, *19*, 156–179.
55. Fernández-García, F.; Martins, M.; Raymond, E.; et al. Unravelling the role of environmentally realistic concentrations of titanium dioxide nanoparticles in altering gametogenesis and gonadal health of female Pacific oysters (*Magallana gigas*): A

histopathological approach. *Aquat. Toxicol*. **2025**, *287*, 107539.
56. Huang, W.; Zhou, Y.; Zhao, T.; et al. The effects of copper ions and copper nanomaterials on the output of amino acids from marine microalgae. *Environ. Sci. Pollut. Res*. **2022**, *29*, 9780–9791.
57. Shang, Y.; Wu, F.; Wei, S.; et al. Specific dynamic action of mussels exposed to TiO_2 nanoparticles and seawater acidification. *Chemosphere* **2020**, *241*, 125104.
58. Huang, X.; Liu, Z.; Xie, Z.; et al. Oxidative stress induced by titanium dioxide nanoparticles increases under seawater acidification in the thick shell mussel Mytilus coruscus. *Mar. Environ. Res*. **2018**, *137*, 49–59.
59. Canesi, L.; Fabbri, R.; Gallo, G.; et al. Biomarkers in *Mytilus galloprovincialis* exposed to suspensions of selected nanoparticles (Nano carbon black, C60 fullerene, Nano-TiO_2, Nano-SiO_2). *Aquat. Toxicol*. **2010**, *100*, 168–177.
60. D'Agata, A.; Fasulo, S.; Dallas, L.J.; et al. Enhanced toxicity of 'bulk' titanium dioxide compared to 'fresh' and 'aged' nano-TiO_2 in marine mussels (*Mytilus galloprovincialis*). *Nanotoxicology* **2014**, *8*, 549–558.
61. Xia, B.; Chen, B.; Sun, X.; et al. Interaction of TiO_2 nanoparticles with the marine microalga *Nitzschia closterium*: Growth inhibition, oxidative stress and internalization. *Sci. Total Environ*. **2015**, *508*, 525–533.
62. Li, S.; Pan, X.; Wallis, L.K.; et al. Comparison of TiO_2 nanoparticle and graphene − TiO_2 nanoparticle composite phototoxicity to *Daphnia magna* and *Oryzias latipes*. *Chemosphere* **2014**, *112*, 62–69.
63. Sanches, M.V.; Oliva, M.; De Marchi, L.; et al. Ecotoxicological screening of UV-filters using a battery of marine bioassays. *Environ. Pollut*. **2021**, *290*, 118011.
64. Roger, L.M.; Adarkwa Darko, Y.; Bernas, T.; et al. Evaluation of fluorescence-based viability stains in cells dissociated from scleractinian coral *Pocillopora damicornis*. *Sci. Rep*. **2022**, *12*, 15297.
65. Wong, S.W.Y.; Zhou, G.-J.; Kwok, K.W.H.; et al. In vivo toxicities of nine engineered nano metal oxides to the marine diatom *Skeletonema costatum* and rotifer *Brachionus koreanus*. *Mar. Pollut. Bull*. **2020**, *153*, 110973.
66. Galletti, A.; Seo, S.; Joo, S.H.; et al. Effects of titanium dioxide nanoparticles derived from consumer products on the marine diatom *Thalassiosira pseudonana*. *Environ. Sci. Pollut. Res*. **2016**, *23*, 21113–21122.
67. Sarkheil, M.; Johari, S.A.; An, H.J.; et al. Acute toxicity, uptake, and elimination of zinc oxide nanoparticles (ZnO NPs) using saltwater microcrustacean, *Artemia franciscana*. *Environ. Toxicol. Pharmacol*. **2018**, *57*, 181–188.
68. Schiavo, S.; Oliviero, M.; Li, J.; et al. Testing ZnO nanoparticle ecotoxicity: Linking time variable exposure to effects on different marine model organisms. *Environ. Sci. Pollut. Res*. **2018**, *25*, 4871–4880.
69. Dobretsov, S.; Sathe, P.; Bora, T.; et al. Toxicity of different zinc oxide nanomaterials at 3 trophic levels: Implications for development of low-toxicity antifouling agents. *Environ. Toxicol. Chem*. **2020**, *39*, 1343–1354.
70. Ates, M.; Daniels, J.; Arslan, Z.; et al. Comparative evaluation of impact of Zn and ZnO nanoparticles on brine shrimp (*Artemia salina*) larvae: Effects of particle size and solubility on toxicity. *Environ. Sci. Process. Impacts* **2013**, *15*, 225–233.
71. Xu, J.; Xin-Ming, P.U.; Lu, D.; et al. Seawater quality criteria and ecotoxicity risk assessment of zinc oxide nanoparticles based on data of resident marine organisms in China. *Sci. Total Environ*. **2023**, *905*, 166690.
72. Byeon, E.; Sanpradit, P.; Lee, J.-S.; et al. Size-dependent toxicity of nano- and microplastics with zinc oxide nanoparticles in the marine rotifer *Brachionus koreanus*. *Mar. Pollut. Bull*. **2024**, *209*, 117206.
73. Suman, T.Y.; Radhika Rajasree, S.R.; Kirubagaran, R. Evaluation of zinc oxide nanoparticles toxicity on marine algae chlorella vulgaris through flow cytometric, cytotoxicity and oxidative stress analysis. *Ecotoxicol. Environ. Saf*. **2015**, *113*, 23–30.
74. Vimercati, L.; Cavone, D.; Caputi, A.; et al. Nanoparticles: An experimental study of zinc nanoparticles toxicity on marine crustaceans. General overview on the health implications in humans. *Front. Public Health* **2020**, *8*, 192.
75. Fabrega, J.; Tantra, R.; Amer, A.; et al. Sequestration of zinc from zinc oxide nanoparticles and life cycle effects in the sediment dweller amphipod *Corophium volutator*. *Environ. Sci. Technol*. **2012**, *46*, 1128–1135.
76. Noventa, S.; Hacker, C.; Rowe, D.; et al. Dissolution and bandgap paradigms for predicting the toxicity of metal oxide nanoparticles in the marine environment: An *in vivo* study with oyster embryos. *Nanotoxicology* **2018**, *12*, 63–78.
77. Trevisan, R.; Delapedra, G.; Mello, D.F.; et al. Gills are an initial target of zinc oxide nanoparticles in oysters *Crassostrea gigas*, leading to mitochondrial disruption and oxidative stress. *Aquat. Toxicol*. **2014**, *153*, 27–38.
78. Miller, R.J.; Lenihan, H.S.; Muller, E.B.; et al. Impacts of metal oxide nanoparticles on marine phytoplankton. *Environ. Sci. Technol*. **2010**, *44*, 7329–7334.
79. Aravantinou, A.F.; Tsarpali, V.; Dailianis, S.; et al. Effect of cultivation media on the toxicity of ZnO nanoparticles to freshwater and marine microalgae. *Ecotoxicol. Environ. Saf*. **2015**, *114*, 109–116.
80. Cuccaro, A.; Oliva, M.; De Marchi, L.; et al. Biochemical response of *Ficopomatus enigmaticus* adults after exposure to organic and inorganic UV filters. *Mar. Pollut. Bull*. **2022**, *178*, 113601.
81. Prato, E.; Fabbrocini, A.; Libralato, G.; et al. Comparative toxicity of ionic and nanoparticulate zinc in the species *Cymodoce truncata*, *Gammarus aequicauda* and *Paracentrotus lividus*. *Environ. Sci. Pollut. Res*. **2021**, *28*, 42891–42900.
82. Zhu, X.; Tan, L.; Zhao, T.; et al. Alone and combined toxicity of ZnO nanoparticles and graphene quantum dots on microalgae *Gymnodinium*. *Environ. Sci. Pollut. Res*. **2022**, *29*, 47310–47322.
83. Zhang, C.; Wang, J.; Tan, L.; et al. Toxic effects of nano-ZnO on marine microalgae *Skeletonema costatum*: Attention to the

accumulation of intracellular Zn. *Aquat. Toxicol*. **2016**, *178*, 158–164.
84. Wu, F.; Sokolova, I.M. Immune responses to ZnO nanoparticles are modulated by season and environmental temperature in the blue mussels *Mytilus edulis*. *Sci. Total Environ.* **2021**, *801*, 149786.
85. Falfushynska, H.I.; Wu, F.; Ye, F.; et al. The effects of ZnO nanostructures of different morphology on bioenergetics and stress response biomarkers of the blue mussels *Mytilus edulis*. *Sci. Total Environ*. **2019**, *694*, 133717.
86. Li, J.; Schiavo, S.; Xiangli, D.; et al. Early ecotoxic effects of ZnO nanoparticle chronic exposure in Mytilus galloprovincialis revealed by transcription of apoptosis and antioxidant-related genes. *Ecotoxicology* **2018**, *27*, 369–384.
87. Muller, E.B.; Hanna, S.K.; Lenihan, H.S.; et al. Impact of engineered zinc oxide nanoparticles on the energy budgets of *Mytilus galloprovincialis*. *J. Sea Res*. **2014**, *94*, 29–36.
88. Ishwarya, R.; Vaseeharan, B.; Subbaiah, S.; et al. Sargassum wightii-synthesized ZnO nanoparticles – from antibacterial and insecticidal activity to immunostimulatory effects on the green tiger shrimp *Penaeus semisulcatus*. *J. Photochem. Photobiol. B: Biol*. **2018**, *183*, 318–330.
89. Wong, S.W.Y.; Leung, P.T.Y.; Djurišić, A.B.; et al. Toxicities of nano zinc oxide to five marine organisms: Influences of aggregate size and ion solubility. *Anal. Bioanal. Chem*. **2010**, *396*, 609–618.
90. Spisni, E.; Seo, S.; Joo, S.H.; et al. Release and toxicity comparison between industrial- and sunscreen-derived nano-ZnO particles. Int. J. *Environ. Sci. Technol*. **2016**, *13*, 2485–2494.
91. Yung, M.M.N.; Kwok, K.W.H.; Djurišić, A.B.; et al. Influences of temperature and salinity on physicochemical properties and toxicity of zinc oxide nanoparticles to the marine diatom *Thalassiosira pseudonana*. *Sci. Rep*. **2017**, *7*, 3662.
92. Bielmyer-Fraser, G.K.; Jarvis, T.A.; Lenihan, H.S.; et al. Cellular partitioning of nanoparticulate versus dissolved metals in marine phytoplankton. *Environ. Sci. Technol*. **2014**, *48*, 13443–13450.
93. Yi, X.; Zhang, K.; Han, G.; et al. Toxic effect of triphenyltin in the presence of nano zinc oxide to marine copepod *Tigriopus japonicus*. *Environ. Pollut*. **2018**, *243*, 687–692.
94. Park, J.; Kim, S.; Yoo, J.; et al. Effect of salinity on acute copper and zinc toxicity to *Tigriopus japonicus*: The difference between metal ions and nanoparticles. *Mar. Pollut. Bull*. **2014**, 85, 526–531.
95. Gelabert, A.; Sivry, Y.; Ferrari, R.; et al. Uncoated and coated ZnO nanoparticle life cycle in synthetic seawater. *Environ. Toxicol. Chem.* **2014**, *33*, 341–349.
96. Cong, Y.; Jin, F.; Wang, J.; et al. The embryotoxicity of ZnO nanoparticles to marine medaka, *Oryzias melastigma*. *Aquat. Toxicol.* **2017**, *185*, 11–18.
97. Jiang, C.; Aiken, G.R.; Hsu-Kim, H. Effects of natural organic matter properties on the dissolution kinetics of zinc oxide nanoparticles. *Environ. Sci. Technol*. **2015**, *49*, 11476–11484.
98. Gomez-Gonzalez, M.A.; Silva-Ferreira, D.T.; Clark, N.; et al. Toward understanding the environmental risks of combined microplastics/nanomaterials exposures: Unveiling ZnO transformations after adsorption onto polystyrene microplastics in environmental solutions. *Glob. Chall.* **2023**, *7*, 2300036.
99. Kaddouri, A.; Serier, B.; Kaddouri, K.; et al. Experimental analysis of the physical degradation of polymers – The case of polymethyl methacrylate. *Fract. Struct. Integr.* **2020**, *14*, 66–80.
100. Dovzhenko, N.V.; Chelomin, V.P.; Kukla, S.P.; et al. Enhanced toxicity of polymethylmethacrylate microparticles on cells and tissue of the marine mussel *Mytilus trossulus* after UV irradiation. *Toxics* **2025**, *13*, 818.
101. Sarkhel, R.; Sengupta, S.; Das, P.; et al. Biodegradation of plastic waste using marine micro-organisms. In *Urban Mining and Sustainable Waste Management*; Ghosh, S.K. Ed.; Springer: Singapore, 2020; pp. 195–201.